Theory of X-ray natural circular dichroism

Ch. Brouder,[a]* C.R. Natoli,[b] Ph. Sainctavit,[a]
J. Goulon,[c] Ch. Goulon-Ginet[c,d] and
A. Rogalev[c]

[a]*Laboratoire de minéralogie-cristallographie, 4 place
Jussieu, 75252 Paris cedex 05, France,* [b] *Laboratori
Nazionali di Frascati dell'INFN, P.O. Box 13, I-00044
Frascati, Italy,* [c] *ESRF,B.P.220, F-38043, Grenoble cedex,
France, and* [d] *Université Joseph Fourier 1 - Faculté de
Pharmacie, B.P.53, F-38041 Grenoble cedex 9, France.
E-mail: brouder@lmcp.jussieu.fr*

A theoretical approach is presented to calculate the natural circular
dichroism recently discovered in the x-ray range (XNCD). XNCD is
shown to be due to an interference of electric dipole and quadrupole
transitions. The basic formula represents XNCD as an odd second-
rank tensor. The crystal symmetries compatible with XNCD are de-
termined. Sum rules are derived that relate XNCD to the mixing of
odd and even orbitals on the absorbing site in the ground state. A
multiple-scattering theory of XNCD is presented. The results are
analyzed to show that XNCD is sensitive to the relative orientation
of the cluster shells. A scattering path analysis is carried out to iden-
tify the paths responsible for the signal.

**Keywords: Keywords: natural circular dichoism, multiple
scattering, sum rule.**

1. Introduction

The idea that interference between electric dipole and electric
quadrupole transitions gives rise to natural circular dichroism in
the x-ray range was put forward in 1988 (Goulon, 1989). The va-
lidity of this idea was confirmed by recent experiments (Goulon
et al., 1998; Alagna *et al.*, 1998) and calculations (Natoli *et al.*,
1998). We refer to Natoli *et al.* (1998) for the full detail and com-
plete formulas concerning XNCD. In the present article, we sacri-
fice generality for clarity, and hope to bring more insight into the
physics of XNCD. First, we describe the relation between natu-
ral circular dichroism and dipole-quadrupole interference, then we
compare the multi-electronic and the mono-electronic sum rules,
we describe the clusters that give rise to XNCD and we investigate
the convergence of the multiple-scattering series of XNCD.

2. Origin of x-ray natural circular dichroism

Electric dipole and quadrupole transitions are well documented in
the x-ray range. Therefore, it would seem natural that interferences
between dipole and quadrupole transitions be larger than pure
quadrupole transitions. Why have these interferences escaped no-
tice until recently ? The absorption cross-section including dipole
and quadrupole transitions is proportional to the sum over final
states of $|\langle f|\epsilon \cdot \mathbf{r}|g\rangle + (i/2)\langle f|\epsilon \cdot \mathbf{r}\mathbf{k} \cdot \mathbf{r}|g\rangle|^2$ (Brouder, 1990).
In a non-magnetic sample, the ground and excited wavefunctions
$|g\rangle$ and $|f\rangle$ can be chosen real. Thus, if the x-rays are linearly po-
larized, ϵ is real, the dipole and quadrupole contributions are in
quadrature: they do not interfere. In other words, the interference

term is observable only with circularly polarized light and the mea-
surement of XNCD had to await the development of reliable circu-
larly polarized sources.

In the optical range, natural circular dichroism is dominated by
the interference of electric dipole and magnetic dipole transitions.
In the x-ray range, magnetic dipole transitions have not been ob-
served unambiguously.

For fully circularly polarized x-rays directed along the z-axis,
the XNCD cross-section is

$$\sigma \ \propto \ \sum_f [\langle g|x|f\rangle\langle f|yz|g\rangle - \langle g|y|f\rangle\langle f|xz|g\rangle]$$
$$\times \delta(E_f - E_g - \hbar\omega).$$

It can be checked that this cross section is zero if the sample has
one of the following symmetries: a center of inversion, a mirror
plane containing the z-axis or a mirror plane perpendicular to the
z-axis.

3. Cross-densities and XNCD sum rules

A density of states is a scalar describing the number of states of a
given symmetry, for instance the K-edge absorption spectrum of a
powder sample measures, up to a matrix element, the density of p-
states of the absorbing atom. However, the development of dichroic
spectroscopies reveals the properties, not only of the number (den-
sity) of states, but also of the states themselves through the projec-
tion operator

$$P(E) = \sum_\phi |\phi\rangle\delta(E - E_\phi)\langle\phi|.$$

The density of p states is the scalar $n_p(E) = \langle x|P(E)|x\rangle +
\langle y|P(E)|y\rangle + \langle z|P(E)|z\rangle$. The various dichroisms give informa-
tion on the non-diagonal elements of $P(E)$, or cross density of
states. For instance, at the K-edge, magnetic circular dichroism is
proportional to a vector (the dipole moment of the p shell) with
z-component $m_z(E) = \langle x|P(E)|y\rangle - \langle y|P(E)|x\rangle$, natural lin-
ear dichroism is proportional to a rank 2 tensor (the quadrupole
moment of the p shell) with elements such as $\langle x|P(E)|x\rangle -
\langle y|P(E)|y\rangle$. Natural circular dichroism at the K-edge is propor-
tional to some non-diagonal matrix elements of $P(E)$ between p
and d states. More precisely, XNCD is proportional to a rank 2
tensor (that we call the p-d cross density of states) with elements
such as $M(E) = \langle x|P(E)|yz\rangle - \langle y|P(E)|xz\rangle$. Contrary to the
quadrupole moment, this rank 2 tensor is odd under inversion.

The relation between the dichroic cross-sections and various
ground state properties are established through sum rules. We
describe now two multi-electronic and one mono-electronic sum
rules. The first multi-electronic sum rule concerns the sum over the
all the edges and reads

$$\int \frac{\sigma}{(\hbar\omega)^2} d(\hbar\omega) \propto \langle g|M|g\rangle$$

where $|g\rangle$ is the multi-electronic ground state and M is the mixing
operator

$$M = \sum_{i,j=1}^{N} z_i(x_iy_j - y_ix_j).$$

N is the number of electrons. Note that $\langle g|M|g\rangle = 0$ for a config-
uration containing only one electron or one hole in an open shell.

The second multi-electronic sum rule can be derived for each edge selectively (Natoli *et al.*, 1998). For a K- or L_I-edge it is

$$\int \frac{\sigma}{(\hbar\omega)^2} d(\hbar\omega) \propto \langle g|M_{pd}|g\rangle$$

where $M_{pd} = a_{xz}^+ a_y - a_{yz}^+ a_x$ in second quantized form. M_{pd} cannot be written as a linear combination of spherical harmonics, because the latter do not mix different orbitals. Notice that the operator M_{pd} does not look Hermitian. However, since the wavefunctions are real, $\langle g|M_{pd}|g\rangle$ is real.

Finally, it is possible to derive an alternative sum rule corresponding to a one-electron model. The one-electron formula for XNCD can be given in terms of the Green function G as

$$\sigma \propto \langle \phi_0|x'\mathrm{Im}[G(\mathbf{r}',\mathbf{r})]yz|\phi_0\rangle - \langle \phi_0|y'\mathrm{Im}[G(\mathbf{r}',\mathbf{r})]xz|\phi_0\rangle,$$

where $|\phi_0\rangle$ is the s core-state of the K- or L_I-edge absorption process. Using the operator identity

$$\int_{-\infty}^{+\infty} dE G(\mathbf{r}',\mathbf{r};E) = -\frac{i}{\pi}\delta(\mathbf{r}'-\mathbf{r}),$$

we obtain the sum rule

$$\int_{-\infty}^{+\infty} d\hbar\omega \frac{\sigma(\omega)}{(\hbar\omega)^2} = 0,$$

which does not assume that the electric dipole and quadrupole reduced matrix elements are constant. However, the integral must be carried out over the whole energy range (of occupied and unoccupied states). Therefore, the sum rule says that the experimental sum over the unoccupied states is equal to minus the sum over occupied states, which is the quantity of interest.

It has already been observed for magnetic circular dichroism, that the dichroic spectrum is proportional to the orbital momentum at all energies in a one-electron approach (Wu *et al.*, 1993). As shown in fig.1, the same behaviour is observed for natural circular dichroism, and the XNCD spectrum is proportional to the p-d cross density of states at all energies. Therefore, the sum over energy of the XNCD spectrum is proportional to

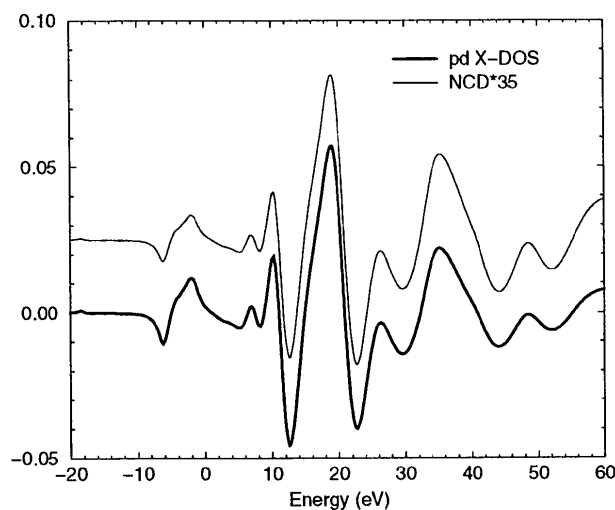$$-\int_{-\infty}^{E_F} dE\langle x|P(E)|yz\rangle - \langle y|P(E)|xz\rangle.$$

Figure 1
Comparison of XNCD at the L_I-edge of I in $LiIO_3$ with p-d cross-density of states.

A similar procedure can be applied to derive one-electron sum rules for other moments of the XNCD spectrum

$$\int_{-\infty}^{+\infty} d\hbar\omega\sigma(\omega)(\hbar\omega)^n,$$

but these moments are not very interesting in the x-ray range, because the edge energy is much larger than the energy range over which XNCD is visible, and the various moments differ essentially by a power of $\hbar\omega_{edge}$.

4. Multiple-scattering interpretation

In Natoli *et al.* (1998), the L_I-edge of iodine in $LiIO_3$ was calculated for a cluster of 40 atoms around iodine, and found in agreement with experiment. However, such a cluster is too large to give us a clear image of what is going on. What are the most important contributions to XNCD in the cluster ?

In the experiments the x-ray beam was along the c-axis of the crystal, which is also the rotation axis of the C_3 point group of iodine. This orientation was chosen to avoid linear dichroism. The measurement of XNCD is much more complex in the presence of linear dichroism, as was analyzed by Goulon *et al.* (1999).

All the shells of equivalent atoms in the cluster have three atoms. Figure 2 shows the first three shells around iodine.
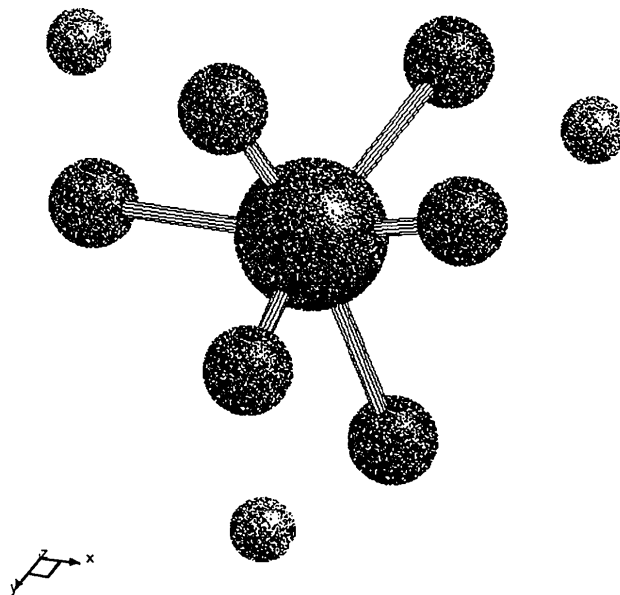

Figure 2
The first two shells (oxygen) around the iodine atom and the third shell of lithium. The c-axis points perpendicular to the page.

With the x-ray beam along the c-axis, none of these shells gives, alone, a contribution to XNCD. This is because any shell of three atoms has a mirror symmetry plane containing the iodine atom and the x-ray beam direction. Thus, because of the symmetry conditions of XNCD, the contribution of each shell is zero and two shells at least are required to produce an XNCD signal. The first two shells of neighbours (three oxygens at 1.803Å and three oxygens

at 2.908Å) give a contribution because the two equilateral triangles of oxygens are rotated respective to one another by an angle different from 0 and π. Therefore, there is no mirror plane common to the two shells, and the first two shells create a major contribution to the XNCD signal (see fig. 3).
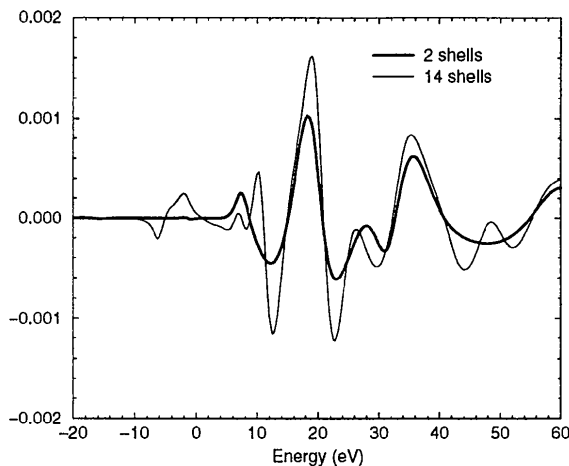

Figure 3
Comparison of XNCD at the L_I-edge of I in $LiIO_3$ for 2 and 14 shells. The main features are broadly reproduced by the interaction of the first two shells.

5. Path analysis

This shows once again that XNCD is a very sensitive probe of local symmetry, since it depends on the relative orientation of the first two shells. It is tempting to investigate the XNCD signal in terms of n-fold scattering paths. It was already noticed that XNCD has no atomic contribution and no single-scattering contribution (Natoli *et al.*, 1998). Therefore, in that sense, XNCD is a purely multiple-scattering phenomenon. However, a scattering-path analysis of XNCD must be carried out with care, because any path can be compensated by its mirror image. The double-scattering and triple-scattering contributions for the first two shells are given in fig. 4. The only paths that contribute to the double-scattering signal are those which go through one oxygen of the first shell and one of the second shell.

6. Conclusion

XNCD is an emerging technique, and much work is still to be done to gain a full understanding of its capabilities. Its relations to non-linear optics and optical spectroscopy have been mentioned in Natoli *et al.* (1998), but other domains of physics will probably be investigated with this technique.

Here, a small step was made towards a better understanding of the origin and physical aspects of XNCD.

Finally, it can be noticed that an alternative way of detecting the interference between electric dipole and quadrupole transitions would be to use complex wavefunctions, i.e. to measure magnetic materials.
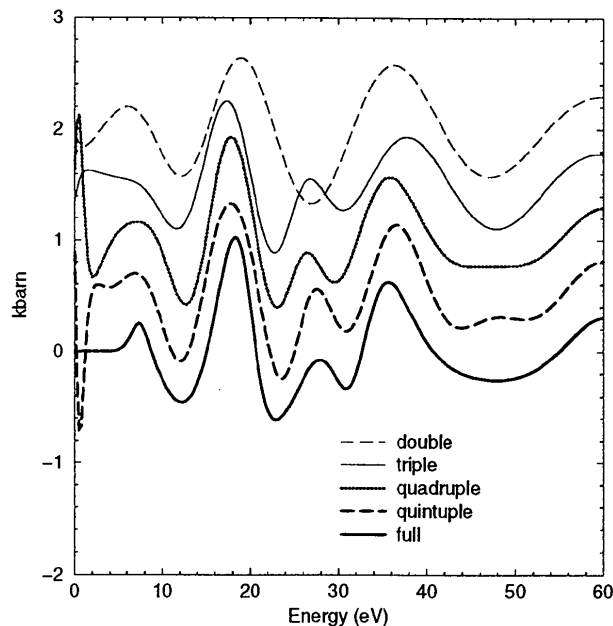

Figure 4
Multiple-scattering expansion for the first two shells (of oxygen) around iodine in $LiIO_3$. The cluster has seven atoms.

References

Alagna, L., Prosperi, T., Turchini, S., Goulon, J., Rogalev, A., Goulon-Ginet, C., Natoli, C., Peacock, R. & Stewart, B. (1998). *Phys. Rev. Lett.* **80**, 4799–802.

Andersen, O. & Jepsen, O. (1984). *Phys. Rev. Lett.* **53**, 2571–4.

Brouder, C. (1990). *J. Phys.: Condens. Matter*, **2**, 597–8.

Goulon, J. (1989). In *Rayonnement synchrotron polarisé, électrons polarisés et magnétisme*, edited by E. Beaurepaire, B. Carrière & J.-P. Kappler, pp. 333–86. Strasbourg: IPCMS.

Goulon, J., Goulon-Ginet, C., Rogalev, A., Gotte, V., Brouder, C. & Malgrange, C. (1999). *J. Opt. Soc. Am. B*, **??**, ??–??

Goulon, J., Goulon-Ginet, C., Rogalev, A., Gotte, V., Malgrange, C. & Brouder, C. (1998). *J. Chem. Phys.* **108**, 6394–403.

Natoli, C., Brouder, C., Sainctavit, P., Goulon, J., Goulon-Ginet, C. & Rogalev, A. (1998). *Euro. Phys. J.* **4**, 1–11.

Wu, R., Wang, D. & Freeman, A. (1993). *Phys. Rev. Lett.* **71**, 3581–4.